LOW INTENSITY NONLINEAR EFFECTS IN COMPTON SCATTERING SOURCES*

F. Albert†, S.G. Anderson, S.M. Betts, R.R. Cross, C.A. Ebbers, D.J. Gibson, T.L. Houck, R.A. Marsh, M. Messerly, S.S. Wu, C.W. Siders, C.P.J. Barty, F.V. Hartemann
LLNL, Livermore, CA, USA

Abstract

The design and optimization of a Mono-Energetic Gamma-Ray (MEGa-Ray) Compton scattering source are presented. A new precision source with up to 2.5 MeV photon energies, enabled by state of the art laser and x-band linac technologies, is currently being built at LLNL. Various aspects of the theoretical design, including dose and brightness optimization, are presented. In particular, while it is known that nonlinear effects occur in such light sources when the laser normalized potential is close to unity, we show that these can appear at lower values of the potential. A three dimensional analytical model and numerical benchmarks have been developed to model the source characteristics, including nonlinear spectra. Since MEGa-ray sources are being developed for precision applications such as nuclear resonance fluorescence, assessing spectral broadening mechanisms is essential.

INTRODUCTION

Nuclear Resonance Fluorescence (NRF) [1] is an isotope specific process in which a nucleus, excited by gamma-rays, radiates high energy photons at a specific energy. This process has been well known for several decades, and has potential high impact applications in homeland security, nuclear waste assay, medical imaging and stockpile surveillance, among other areas of interest. Although several successful experiments have demonstrated NRF detection with broadband bremsstrahlung gamma-ray sources [2], NRF lines are more efficiently detected when excited by narrowband gamma-ray sources. Indeed, the effective width of these lines, $\Delta E/E$, is on the order of 10^{-6}. Currently, Compton scattering is the only physical process capable of producing a narrow bandwidth radiation (below 1%) at gamma-ray energies, with state-of-the art accelerator and laser technologies. In Compton scattering sources, a short laser pulse and a relativistic electron beam collide to yield tunable, monochromatic, polarized gamma-ray photons. Several projects have recently utilized Compton scattering to conduct NRF experiments: Duke university [3], Japan [4] and Lawrence Livermore National Laboratory (LLNL) [5, 6, 7]. In particular, LLNL's Thomson-Radiated Extreme X-rays (T-REX) project demonstrated isotope specific detection of low density materials behind heavier elements [5].

This paper presents, within the context of NRF-based applications, the theoretical and conceptual design of a narrowband monoenergetic gamma-ray (MEGa-ray) source. In particular, weakly nonlinear effects are studied in the picosecond regime.

COMPTON SCATTERING OVERVIEW

The Compton formula can be derived from energy-momentum conservation, and expressed as follows:

$$u_\mu + \lambda k_\mu = v_\mu + \lambda q_\mu \tag{1}$$

Here, u_μ and v_μ are the initial and scattered electron 4-velocities, while k_μ and q_μ are the incident and scattered 4-wavenumbers, respectively. The 4-velocities are normalized, with $u_\mu u^\mu = v_\mu v^\mu = 1$, and the dispersion relation implies that $k_\mu k^\mu = q_\mu q^\mu = 0$. Hence, using these conditions allows for the elimination of the scattered electron 4-velocity, and results in:

$$u_\mu (k^\mu - q^\mu) = \lambda k_\mu q^\mu. \tag{2}$$

Eq. 2 can be also written in a slightly different manner by introducing the incident and scattered light-cone variables [10], $\kappa = u_\mu k^\mu$, and $\lambda = u_\mu q^\mu$, respectively:

$$\kappa - \lambda = \lambda k_\mu q^\mu. \tag{3}$$

Finally, in regular units and 3-vector form: $u_\mu = (\gamma, \mathbf{u})$; $q_\mu = q(1, \mathbf{n})$, where $\mathbf{n}$ is the unit vector along the direction of observation; and $k_\mu = (k, \mathbf{k})$; this yields the well-known Compton formula:

$$\frac{q}{k} = \frac{\gamma - \mathbf{u}.(\mathbf{k}/k)}{\gamma - \mathbf{n}.\mathbf{u} + \lambda(k - \mathbf{n}.\mathbf{k})} \tag{4}$$

Here k is the wave number and $\gamma = 1/\sqrt{1 - v^2/c^2}$ is the electron relativistic factor. In other words:

$$\frac{q}{k} = \frac{\gamma - u\cos\varphi}{\gamma - u\cos\theta + \lambda k[1 - \cos(\theta + \varphi)]}, \tag{5}$$

where φ is the angle between the incident laser and electron and θ is the angle between the incident electron and scattered gamma-ray photon.

* This work performed under the auspices of the U.S. Department of Energy by Lawrence Livermore National Laboratory under Contract DE-AC52-07NA27344.

† albert6@llnl.gov

For realistic laser-electron interactions, one has to take into account the electron phase space and the laser transverse dimensions. The exact nonlinear plane wave solution for the 4-velocity has been derived in earlier work [11, 12, 13]:

$$u_\mu = u_\mu^0 + A_\mu - k_\mu \frac{A_\nu(A^\nu + 2u_0^\nu)}{2k_\nu u_0^\nu}, \tag{6}$$

where u_μ^0 is the initial 4-velocity and A_μ is the laser 4-potential. By using the nonlinear 4-velocity in conjunction with Eq. 2, one obtains:

$$\left(u_\mu^0 + A_\mu - k_\mu \frac{A_\nu A^\nu + 2u_\nu^0 A^\nu}{2u_\nu^0 k^\nu}\right)(k^\mu - q^\mu) = \lambda\!\!\!^{-} k_\mu q^\mu, \tag{7}$$

which, after applying the Lorentz gauge condition $k_\mu A^\mu = 0$, and the dispersion relation in vacuum, $k_\mu k^\mu = 0$, simplifies to:

$$u_\mu^0 k^\mu - \left(u_\mu^0 - \frac{k_\mu}{2u_\nu^0 k^\nu}\langle A_\nu A^\nu\rangle\right) q^\mu = \lambda\!\!\!^{-} k_\mu q^\mu. \tag{8}$$

This new relation is a modified form of the Compton formula, now including the nonlinear ponderomotive force of the laser field. When referring to the geometry described in Fig. 1, Eq. 8 becomes:

$$\frac{q}{k} = \frac{\gamma - u\cos(\epsilon+\varphi)}{\gamma - u\cos(\theta+\epsilon) + (1-\cos(\varphi+\theta+\epsilon))\left[\frac{\langle -A_\mu A^\mu\rangle}{2[\gamma - u\cos(\varphi+\epsilon)]} + \lambda\!\!\!^{-} k\right]}. \tag{9}$$

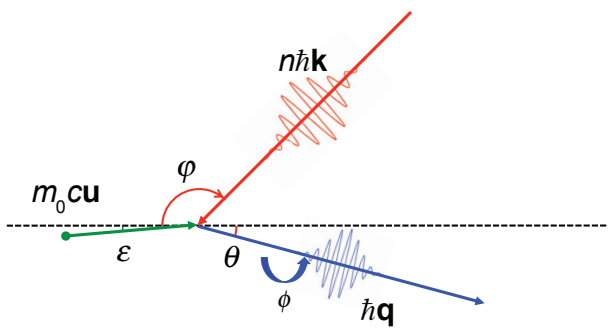

Figure 1: Definition of the Compton scattering geometry in the case of an electron beam.

Here the small angle ϵ is different for each electron and represents the emittance of the electron beam. Note also that $\langle -A_\mu A^\mu\rangle$ is the nonlinear radiation pressure. By looking at the variation of q as a function of all the parameters in Eq. 9, for on-axis observation ($\theta = 0$) one finds that $\Delta q/q \propto \Delta k/k$, $\Delta q/q \propto -\frac{1}{4}\Delta\varphi^2$, $\Delta q/q \propto 2\Delta\gamma/\gamma$, $\Delta q/q \propto -\gamma^2\Delta\epsilon^2$, and $\Delta q/q \propto -\frac{\Delta A^2}{1+A^2}$. While the gamma ray spectral width depends directly on the electron and laser energy spreads, it is also strongly affected by the electron beam emittance because of the γ^2 factor. This provides a quick overview of the various sources of spectral broadening in a Compton scattering light source. Note that the negative variations are asymmetric broadening toward lower photon energies.

WEAKLY NONLINEAR EFFECTS

To accurately simulate realistic interactions between a high brightness electron beam and a laser pulse, and study their influence on high-precision Compton scattering light sources, a fully 3D code is required. For long, narrow-band laser pulses, a direct approach, accounting for fine details in the correlated electron beam phase space, is computationally intensive. Instead, one can take advantage of the slow-varying pulse envelope, paraxial, and weakly nonlinear approximations to develop a local plane-wave model leading to analytical expressions for the electron 4-trajectory. The corresponding three small parameters are: $\Delta\phi^{-1}$,$\epsilon = (k_0 w_0)^{-1}$, and A_0 , respectively. For large Doppler upshifts, these conditions ensure that the particle excursions from ballistic trajectories are very small compared to all other scales characterizing the system. In turn, this allows the use of a local plane wave model, where all dynamical variables become functions of ϕ : the 6-dimensional input phase space specifies a ballistic trajectory for a given electron,$x_\mu^i(\phi) = x_\mu^{0i} + \phi(u_\mu^{0i}/\kappa_i)$; all other dynamical quantities are evaluated along this 4-trajectory.

The three-dimensional electromagnetic fields are generated from the vector $\mathbf{G}$, by taking $\mathbf{A} = \nabla\times\mathbf{G}$, thus ensuring a divergence-free potential vector satisfying the Coulomb gauge. The electric field is given by $\mathbf{E} = -\partial_t\mathbf{A}$, while the magnetic induction is $\mathbf{B} = \nabla\times A$. In the case of a Gaussian pulse propagating paraxially along the positive z-axis, focused cylindrically, and polarized along the x-axis, the generating function is [14]:

$$G_y = \frac{A_0 e^{-\frac{\phi^2}{\Delta\phi^2} - \frac{r^2}{1+z^2}} \cos\left[-\phi - z\frac{r^2}{1+z^2} - \mathrm{atan}(z)\right]}{k_0\sqrt{1+z^2}}. \tag{10}$$

Here, A_0 is the amplitude of the vector potential; $k_0 = \omega_0/c$ is the central wavenumber of the pulse. Space-time coordinates are normalized as follows: $r \to r/w_0$, $z \to z/z_0$, $t \to ct/z_0$, $z_0 = \frac{1}{2}k_0 w_0^2$ is the Rayleigh range, w_0 is the focal waist, $\phi = \omega_0 t - k_0 z$ is the phase, and $\Delta\phi = \omega_0 t$. Using both the slow-varying envelope and the paraxial approximations, and systematically neglecting higher order terms, the 4-potential is derived. Replacing all space-time coordinates by their values along ballistic trajectories, the local 4-velocity can be evaluated by keeping terms of order A_0, $A_0\epsilon$, ϵ, and A_0^2; for example, the component parallel to the polarization, is:

$$u_x(\phi) = u_{x0} + A_0 \frac{\exp\left[-\frac{\phi^2}{\Delta\phi^2} - \frac{r(\phi)^2}{1+z(\phi)^2}\right]}{\sqrt{1+z(\phi)^2}} \tag{11}$$

$$\times\left[1+4\epsilon\frac{u_{x0}}{\gamma_0-u_{z0}}\frac{x(\phi)z(\phi)}{1+z(\phi)^2}\right]\sin[-\phi-\psi(\phi)],$$

where $\psi=-z[r^2/(1+z^2)]+\text{atan}(z)$.

Beyond this point, the flow of the 3D code, explained in details in Ref. [13], can be summarized as follows. All dynamical quantities are separated into slow-varying components and periodic functions; integrals over the phase are performed using the approximation: $\int f p d\phi \simeq \langle p\rangle \int f d\phi + f\int(p-\langle p\rangle)d\phi$, where $p(\phi+2\pi)=p(\phi)$, and where the average is defined as $\langle p\rangle=\frac{1}{2\pi}\int_{-\pi}^{\pi}pd\phi$. For harmonic functions, $\int(p-\langle p\rangle)d\phi$ is analytical, while the integral over f can be performed efficiently because it is a slow-varying function. This approximation is used to evaluate the 4-trajectory and the radiation integral. For situations dominated by diffraction, the Fourier transform of the asymmetric Lorentzian envelope yields complex nonlinear spectra. Finally, for a 6N-dimensional distribution of input particles in phase space, as shown in Fig. 2, the radiation is obtained by incoherent summation; linear (blue) and nonlinear (red) spectra are shown in Fig. 3. Full 3D trajectories are used for all cases, the linear spectra are calculated from the ballistic phase $\frac{q_\mu}{\kappa}(u_0^\mu+\lambda k^\mu)\phi$ only. Even for $A_0^2=2.5\times10^3<<1$, the difference between linear and nonlinear spectra is clearly established, both for for an idealized electron beam and for a realistic case.

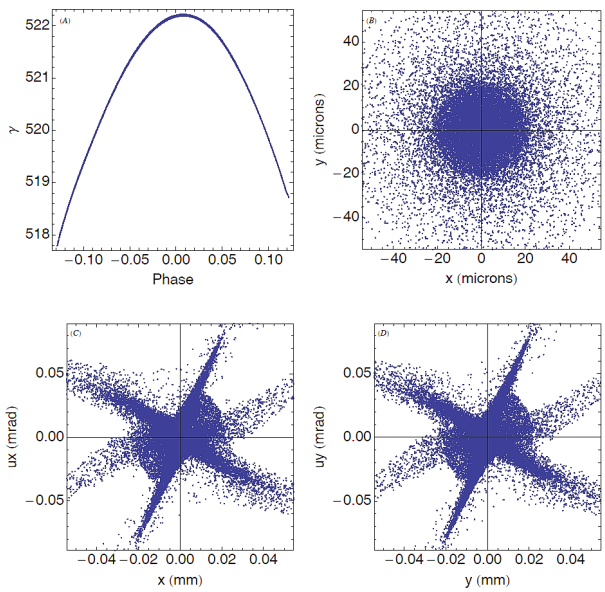

Figure 2: PARMELA electron beam simulations: (A): γ vs. radiofrequency (rf) phase, (B): beam focal spot, (C) and (D): phase space.

CONCLUSION

In this Paper, the theoretical design of narrow-band Compton scattering gamma-ray sources is presented within the specific context of nuclear resonance fluorescence applications. NRF is a very powerful isotope-specific process that has potential high impact applications in homeland security, nuclear waste assay and management, stockpile surveillance or medicine. In order for this process to be fully efficient, it is necessary to operate in a spectrally narrow regime. In order to assess spectral broadening mechanisms in Compton scattering, detailed theory modeling are necessary. Nonlinear, three dimensional effects have to be accounted for when designing high precision narrow-band gamma-ray sources.

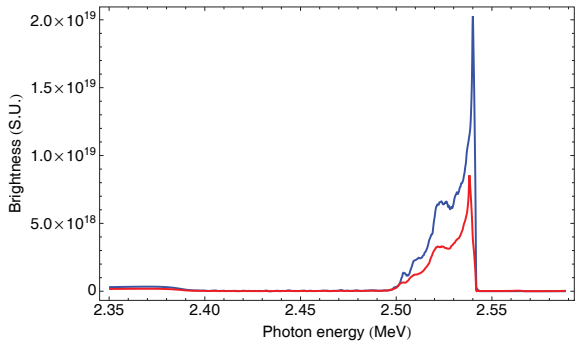

Figure 3: Linear (blue) and nonlinear (red) spectra from the electron distribution of Fig. 2; the laser parameters are: 10 ps FWHM pulse duration, 532 nm wavelength, 12 μm rms spot size, 150 mJ energy.

REFERENCES

[1] U. Kneissl, H.M. Pitz and A. Zilges, Prog. Part. Nucl. Phys., 37, pp 349-433 (1996).

[2] W. Bertozzi, *et al.*, Phys. Rev. C, 78, 041601(R) (2008).

[3] C.A. Hagmann, *et al.*, J. Appl. Phys. 106, 084901 (2009).

[4] N. Kikuzawa, *et al.*, Appl. Phys. Express 2, 036502 (2009).

[5] F. Albert, *et al.*, Opt. Lett, 35, 3 354 (2010).

[6] D. J. Gibson, *et al.*, Phys. Rev. ST Accel. Beams 13, 070703 (2010).

[7] F. Albert, *et al.*, Phys. Rev. ST Accel Beams 13, 070704 (2010).

[8] W. Bertozzi, *et al.*, Nucl. Instrum. Methods Phys. Res. B 261, 331 (2007).

[9] J. Pruet, *et al.*, J. Appl. Phys. 99, 123102 (2006).

[10] L.M. Brown and R.P. Feynmann, Phys. Rev. 85, 231 (1952).

[11] J.W. Meyer, Phys. Rev. D, 3, 621 (1971).

[12] F.V. Hartemann, F. Albert, C.W. Siders and C.P.J. Barty, Phys. Rev. Lett., 105, 130801 (2010).

[13] F. Albert, S.G. Anderson, D.J. Gibson, R.A. Marsh, C.W. Siders, C.P.J. Barty and F.V. Hartemann, Phys. Plasmas, 18, 013108 (2011).

[14] F.V. Hartemann, J.R. Van Meter, A.L. Troha, E.C. Landahl, N.C. Luhmann, Jr., H.A. Baldis, A. Gupta and A.K. Kerman, Phys. Rev. E 58, 5001-5012 (1998).